

An experiment on multiple pathway quantum interference for the advanced undergraduate physics laboratory

Clark Vandam, Aaron Hankin, and A. Sieradzan

Department of Physics, Central Michigan University, Mt. Pleasant, MI 48858

M.D. Havey

*Department of Physics, Old Dominion University, Norfolk, VA 23529**

(Dated: July 25, 2018)

We present results on a multiple-optical-path quantum interference project suitable for the advanced undergraduate laboratory. The experiments combine a conceptually rich set of atomic physics experiments which may be economically developed at a technical level accessible to undergraduate physics or engineering majors. In the experiments, diode-laser driven two-quantum, two-color excitation of cesium atoms in a vapor cell is investigated and relative strengths of the individual hyperfine components in the $6s^2S_{1/2} \rightarrow 7s^2S_{1/2}$ transition are determined. Measurement and analysis of the spectral variation of the two quantum excitation rate clearly shows strong variations due to interfering amplitudes in the overall transition amplitude. Projects such as the one reported here allow small teams of undergraduate students with combined interests in experimental and theoretical physics to construct instrumentation, perform sophisticated experiments, and do realistic modelling of the results.

I. INTRODUCTION

Nonlinear optics has developed into a mature scientific field [1–3], and yet the subject continues to drive investigations into new areas ranging from development of quantum memories and quantum repeaters [4, 5], to novel laser types [6] including random lasers in ultracold atom samples [7]. At the same time, an important emerging approach to physics education has been to place strong emphasis on significant scientific research experiences for undergraduate students. In fact, it is not unusual for undergraduate physics majors to start working in a research laboratory as soon as they begin their education in the university. In this regard, research experiences involving laser based optical sciences are well known to be particularly attractive to undergraduate science students. This is in part because the existing technology is mature, is visible, and at the same time is quite technically and scientifically accessible to physics undergraduates. This fosters relatively rapid independent work in the laboratory, a definite asset to developing interest and practical knowledge in students.

One area of nonlinear optics that is particularly accessible and attractive as a component of undergraduate research is the application and study of two photon processes, which include two-photon resonant and non-resonant absorption, stimulated Raman scattering, and a wide range of coherent processes associated with coherent population trapping. With the pioneering experiments on two-photon absorption within the hyperfine structure of the $5s\ ^2S_{1/2}$ level in the sodium atom [8–10], two-photon spectroscopy established itself as an important experimental spectroscopic technique, routinely

providing sub-Doppler resolution in atomic level structure measurements. With the advent of relatively economical tunable and single mode diode lasers [11, 12], experiments of this kind, often performed with a single light source, have found their way into undergraduate student laboratories [13].

By using two independently tuned diode lasers instead of one, thus performing two-color two-quantum spectroscopy, one can add other degrees of freedom to the experiments, these being the polarization states of the two exciting light sources and an adjustable energy splitting between the two quanta needed to drive the transition. This technique has been utilized in many atomic and molecular physics studies [14–17], including the precise measurement of relative atomic transition probabilities. It has also been the focus of several research projects completed in our laboratory [17–22]. The experiments were motivated primarily by the need for atomic physics benchmarks with which to measure the precision of high level atomic physics structure calculations, particularly in atomic Cs [23, 24]. These relativistic atomic physics calculations, in turn, are essential to interpretation of parity violation measurements in atomic Cs [23–28]. In the series of measurements, two-quantum atomic transitions and their relative strengths as a function of intermediate (virtual) level detuning from the real atomic level were studied, and high precision data on transition matrix elements involving S, P, and D doublets in alkali atoms were obtained. In these experiments it was interplay between the polarization of the exciting light fields and the detuning from one photon resonance that led to the high precision obtained. Physics undergraduate majors and Master of Science students played important roles in several of these projects.

To illustrate the basic ideas, we turn first to Fig. 1, which shows a generic arrangement of four energy levels, and a two-photon excitation scheme. In the scheme, ex-

*Electronic address: mhvey@odu.edu

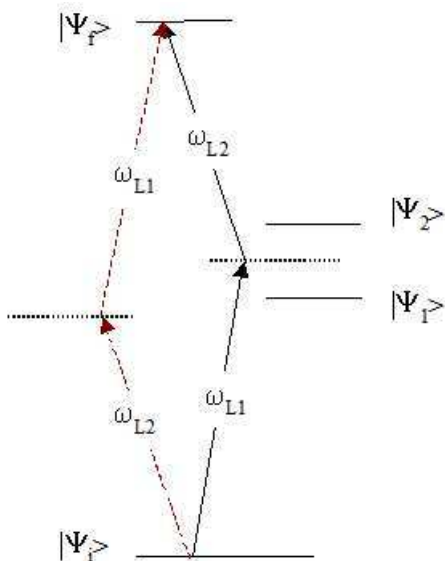


FIG. 1: Generic energy level diagram of selected energetically low-lying atomic energy levels and two-quantum excitation pathways from an initial level to a final level. The wavefunction for the initial level is denoted $|\Psi_i\rangle$, while that for the final level as $|\Psi_f\rangle$. The two intermediate levels are denoted $|\Psi_m\rangle$ with $m = 1, 2$. The frequencies of the two laser light sources exciting the transition are labelled as ω_{Lk} with $k = 1, 2$. Horizontal dotted lines represent the two so-called virtual levels for the transition. Drawing not to scale.

citation is resonant with the two-photon transition $i \rightarrow f$, but not separately resonant with either the first or second steps of the process. Qualitatively, the two photon process, in this case leading to population transfer from the initial to the final level may proceed coherently through either of the two intermediate levels. This by itself leads to interferometric variation of the transition probability as a function of the frequencies of the two light sources. In addition, the two time orders of interaction with the two light sources are coherent with each other, and with the amplitudes for transition through the two intermediate levels. The relative size of these contributions depends on the detuning δ from resonant step-wise absorption, where the two laser sources are frequency tuned to exact resonance with the atomic level separations. In Fig. 1, $\delta = \omega_{L1} - \omega_2$, subject to the constraint that the two photon resonance condition is satisfied: $\omega_{L1} + \omega_{L2} = \omega_f - \omega_i$.

More quantitatively, the relative polarization-dependent, two-photon transition amplitude M_{tp} is given, in the electric dipole approximation, by [29]

$$M_{tp} = \sum_n \left[\frac{\langle \Psi_f | \epsilon_1 \cdot r | \Psi_n \rangle \langle \Psi_n | \epsilon_2 \cdot r | \Psi_i \rangle}{\omega_n - \omega_{L1}} + \frac{\langle \Psi_f | \epsilon_2 \cdot r | \Psi_n \rangle \langle \Psi_n | \epsilon_1 \cdot r | \Psi_i \rangle}{\omega_n - \omega_{L2}} \right] \quad (1.1)$$

In this expression, ϵ_k and ω_{Lk} represent the polariza-

tion vector and the frequency of the light source ($k = 1, 2$). The index n labels the contributing intermediate levels (in Fig. 1, $n = 1, 2$) and their frequencies ω_n . For the two intermediate levels of Fig. 1, there are then four terms in the expression for M_{tp} . The $i \rightarrow f$ transition probability is proportional to $|M_{tp}|^2$, leading in this illustration to 16 contributing interfering terms. We should point out that there are generally an infinite number of contributions associated with off-resonance transitions to more energetic electronic states. These contributions are often small, and where necessary can be estimated through known atomic spectroscopy data.

In many applications, ground state alkali atoms are excited to one of the higher S or D states via a two-quantum process, with an intermediate virtual level in the vicinity of the resonance 2P_j doublet level ($j = 1/2, 3/2$) [30]. Quantum interference between transition amplitudes associated with the two allowed excitation paths is then evident in dramatic changes of overall transition probability, as the detuning varies. From a fluorescence or ionization signal dependence on detuning, the relative transition probabilities for fine structure doublets can be determined. The dependence on the relative polarizations of the two light sources can lead to much greater precision in the relative transition amplitudes, but requires very good experimental control of the laser frequencies and polarizations. As mentioned earlier, this approach has been used to obtain precise relative transition amplitudes in a number of cases [17–22].

We should also point out that interferences between contributing pathways, as appear in Eq. 1, have important applications in the broad field of quantum control of atomic and molecular processes [31–33]. In the present case, the quantum or classical nature of the exciting fields can strongly influence the overall transition rate [29], but this dependence does not appear in the interfering terms in the configuration we consider here. In elaborations of the scheme of Fig. 1, they can be made to appear in interesting ways. For example, addition of a third field connecting one of the levels with $n = 1, 2$ to a yet higher energy level can make the transition amplitude through the $n = 1, 2$ levels more or less distinguishable, and modify the phase and amplitude of one or more of the interfering terms.

In this paper, we present results on a multiple path quantum interference experiment suitable for the advanced undergraduate laboratory. In the experiments, two-quantum, two-color excitation of cesium atoms in a vapor cell is investigated. In particular, the $6s^2S_{1/2} \rightarrow 7s^2S_{1/2}$ transition is studied, and the relative probability of transition to the final $7s^2S_{1/2}$ level is measured as a function of exact frequency offset from resonant two photon excitation. Measurements are made in the vicinity of the $6s^2S_{1/2} \rightarrow 6p^2P_{3/2}$ (D2) transition, in which case the interfering levels (viz. Eq. 1) are the hyperfine components of this transition. The observed strong interference effects are analyzed by accounting for the various contributing transition amplitudes and the

significant Doppler broadening of the transitions. Because of the combination of experimental and analysis components in projects of the type reported here, small teams of undergraduate students with combined interests in experimental and theoretical physics can collaborate in construction of instrumentation, performance of sophisticated experiments, and realistic modelling of the results.

The remainder of this paper is organized as follows. We first provide a sketch of the theoretical results necessary for the interpretation of the measurements and for fitting the observed spectral variations of the two-photon transition rate data. This is followed by a detailed description of the experimental arrangement and protocols, and a discussion of the experimental results. We conclude with a brief summary and perspective on the type of project described here.

II. THEORY

In this section, we present some details of application of the general expression for M_{tp} to the $6s^2S_{1/2} \rightarrow 7s^2S_{1/2}$ transition in atomic Cs. This treatment consists of two broad parts. In the first subsection, we present an illustrative treatment of this transition neglecting hyperfine structure in any of the electronic levels. This allows tracing of the essential steps in the calculation, these being the same for the algebraically more complex case where the hyperfine splitting is included. This approach also turns out to be useful in its own right, as it gives the correct result in the case where the ground level is initially unpolarized and where the offset of the exciting light sources is large compared to the intermediate levels ($6p^2P_{1/2}$ and $6p^2P_{3/2}$ hyperfine structure). In a second subsection, we provide an overview of a more general approach to calculation of M_{tp} . This is followed by presentation of theoretical expressions for the hyperfine-structure dependent spectral variations of the relative two photon transition signals.

As is well known, atomic perturbation theory predicts a nonzero probability for two-quantum electric-dipole transitions between atomic states of the same parity [29, 34]. Starting with an alkali atom in its ground state, for example, higher lying S and D states may be populated by two light sources whose frequencies add to the frequency separation of the initial and final levels. For a naturally broadened transition, theoretical expressions for the transition amplitudes are readily available [29]. These expressions depend on the single photon transition matrix elements between the initial and intermediate levels, and between the intermediate levels and the final selected level. The matrix elements depend sensitively on the polarization of the two light sources used. The amplitudes depend importantly also on the detuning of the lasers from exact one plus one two photon resonance. With reference to Figure 2, this detuning is represented by the offset of Laser 1 from resonance (indicated

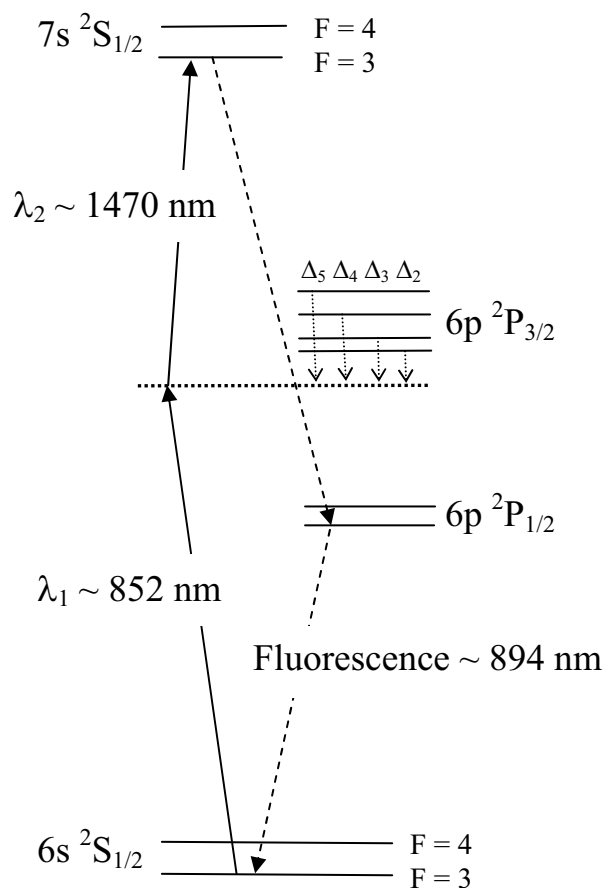


FIG. 2: Schematic energy level diagram of selected energetically low-lying atomic Cs energy levels and two-quantum excitation pathways to the final $7s^2S_{1/2}$ level. The horizontal dotted line represents the main contributing virtual level for the transition. Horizontal lines schematically indicate the hyperfine levels within each indicated atomic electronic level, while vertical dotted lines represent the detuning of the near-resonance virtual level from the various $6p^2P_{3/2}$ hyperfine levels. Not to scale.

by the position of a virtual level) through the $6p^2P_{3/2}$ level. In fact, and in general, for each allowed two photon amplitude, there are two such detunings reflecting the fact that the two temporal orders of photon absorption are indistinguishable. In the general case, there are also many intermediate levels which sensibly contribute to the two photon transition probability. However, the simplest situation occurs when one or several energetically close terms in the summation of the contributions dominate, while the rest contribute at the level of often-negligible corrections. In more typical circumstances, when several atomic levels with comparable detuning are present, the corresponding terms in transition amplitude must be kept and the overall sum squared to obtain the overall transition probability.

To evaluate the intensity ratio for hyperfine line components in two-quantum S-S transition, one needs to know the relevant single photon transition matrix ele-

ments and the detuning values. It is a useful and accessible exercise in introductory quantum mechanics, and in angular momentum coupling rules in particular [35], to obtain the transition amplitudes starting with an alkali atom without spin, then include the effects of the fine structure, and finally consider a real atom with its nuclear spin and the associated hyperfine structure. We have performed such calculations for all permitted S-P transitions in ^{133}Cs , which has a nuclear spin $I = 7/2$. We refer the reader to the excellent summary of transition elements by Steck [36]. The various contributing hyperfine levels, for the transitions specifically considered in the present paper, are shown schematically in Figure 2.

In evaluating two-quantum transition probabilities between specific hyperfine levels (e.g. from the $F = 4$ hyperfine component of the $6s^2S_{1/2}$ ground level to the $F' = 3$ hyperfine level associated with the $7s^2S_{1/2}$ electronic state), we assume equal populations for Zeeman sublevels of the ground state and identical reduced transition matrix elements across the hyperfine manifold. Indistinguishable two-quantum excitation paths have their transition amplitudes added, while transition probabilities are summed for distinguishable paths, and the final result for the total $F \rightarrow F'$ transition probability is obtained. In the following expressions, we neglect the generally interfering contribution from the $6p^2P_{1/2}$ level. We should point out that, for lighter alkali atoms with smaller D-line fine-structure splitting, this is not a very good approximation. In the present case, these variations have a negligible effect on the experimental results. Then excluding common constant factors, the transition probabilities, for perpendicularly polarized excitation beams, are proportional to

$$P_{33} = \frac{34}{63\Delta_2^2} + \frac{35}{128\Delta_3^2} + \frac{125}{896\Delta_4^2} - \frac{1}{6\Delta_2\Delta_3} - \frac{5}{14\Delta_2\Delta_4} - \frac{15}{64\Delta_3\Delta_4} \quad (2.1)$$

$$P_{43} = P_{34} = \frac{21}{128\Delta_3^2} + \frac{119}{384\Delta_4^2} + \frac{7}{64\Delta_3\Delta_4} \quad (2.2)$$

$$P_{44} = \frac{161}{3456\Delta_3^2} + \frac{2009}{9600\Delta_4^2} + \frac{682}{675\Delta_5^2} - \frac{49}{960\Delta_3\Delta_4} - \frac{77}{270\Delta_3\Delta_5} - \frac{77}{150\Delta_4\Delta_5} \quad (2.3)$$

where Δ_F represents the virtual level detuning from individual hyperfine structure sublevels of the $6p^2P_{3/2}$ cesium level. These detunings are indicated schematically in Figure 2. Note that, in practical terms, the detuning of Laser 1 (see Figure 2), labelled for instance as x , is referenced to the frequency of the hyperfine-average $6s^2S_{1/2} \rightarrow 6p^2P_{3/2}$ resonance transitions. Individual Δ_F

are then expressed in terms of x using the known hyperfine level locations. For example, $\Delta_5 = 3758 \text{ MHz} + x$, for excitation from $F = 4$.

In the limit where all detuning become large compared to the hyperfine splittings, and all Δ_F are nearly identical, the ratios of transition probabilities become constant, and are given by $P_{43}/P_{44} = 7/5$ and $P_{34}/P_{33} = 3/1$. In general the spectral dependence of the ratios depends in a complicated way on detuning, but are in any case given by Eq. 2.1 - 2.3, so long as the detunings are all larger than the Doppler and natural widths of the individual hyperfine transitions. These results are valid for ^{133}Cs only, but similar calculations of relative transition probabilities can be easily extended to other systems. Strictly speaking, the above expressions are correct only when the individual transition amplitudes scale as $1/\Delta$, and do not directly apply when the detuning becomes on the order of the natural width of any of the individual hyperfine resonances. How wide a spectral range needs to be so that these expressions apply depends on the natural width of the transitions and on the temperature of the sample. For experiments performed with cold atoms [8], the natural width of a few MHz would determine the "resonance region". In the case considered here, where a cesium vapor was kept at 323 K, the Doppler broadened resonance frequencies spread over hundreds of megahertz and to produce theoretical curves to compare with experimental intensity ratios, one needs first to integrate the transition probability expressions over the Doppler distributed resonance frequencies, and then make proper comparisons between theory and experiment outside the Doppler width range of about 500 MHz around the center of each resonance. Results obtained from such a procedure are used for comparison with experimental data in the following sections of the paper.

III. EXPERIMENTAL DESCRIPTION AND PROTOCOLS

The experimental arrangement is shown schematically in Figure 3. Excitation of Cs to the $7s^2S_{1/2}$ level is achieved by means of two independently tuned, extended-cavity diode lasers. Each laser operates on a single longitudinal mode, and provides a few milliwatts of output power. A fraction of this intensity, depending on detuning from hyperfine resonance, was used to excite the Cs atoms to the $7s^2S_{1/2}$ state. The linearly laser beams pass through optical isolators, after which they are polarized orthogonal to each other. They are then directed, in a counter-propagating fashion, through a Pyrex glass cell with flat windows containing saturated cesium vapor at an equilibrium cell temperature stabilized to 323(1) K, maintaining a cesium vapor pressure of about 10^{-5} Torr. To avoid two-photon transition saturation, and preserve good collimation of the beams, no focusing lens is used in either of the beams. In addition to this precaution, neutral density filters are inserted in the beams when either

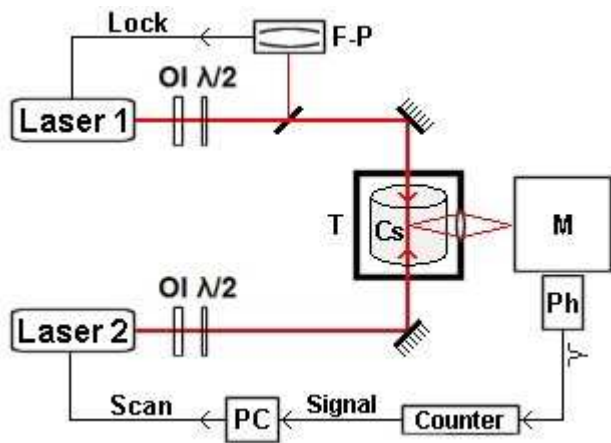


FIG. 3: Schematic diagram of the experimental apparatus. Abbreviations in the figure correspond to OI (optical isolator), $\lambda/2$ (half-wave retardation plate), T (sample cell oven), M (monochromator), Ph (photomultiplier tube), PC (data acquisition computer, F-P (Fabry-Perot interferometer), and Cs (the atomic Cs vapor cell).

laser frequency approaches single photon resonance.

Atomic population in the $7s^2S_{1/2}$ level is monitored by the cascade fluorescence through the $6p^2P_{1/2}$ level at 894 nm (the Cs D1 line). The fluorescence light from the cell is spectrally filtered by a 0.5m double monochromator, and detected with a gallium arsenide photocathode photomultiplier operating in a photon-counting mode.

The first laser has its wavelength set at the beginning of each run. The virtual level detuning from the $6p^2P_{3/2}$ level resonance is determined by counting transmission cycles in a confocal Fabry-Perot interferometer (which has a free spectral range of 2 GHz), observed during the laser frequency adjustment starting at the point of maximum absorption of an attenuated beam in an auxiliary room-temperature Cs reference cell. Comparison with a more elaborate saturated absorption scheme allowed us to determine that such a simple reference results in laser frequency determination and reproduction with an accuracy of about ± 60 MHz, more than adequate for the present experiment.

After the initial adjustment, the frequency of laser 1 is electronically locked to a transmission peak in the interferometer. The frequency stability of the lock, with the interferometer contained in a thermally insulated enclosure without active temperature stabilization, is 50 MHz or better for the typical one-hour duration of a run. The overall quadrature laser 1 frequency determination error is then ± 80 MHz. The second diode laser, laser 2, has its frequency scanned in a narrow range over which two-quantum resonances are observed. Relative intensities of the four excitation/fluorescence peaks, which correspond to different F, F' combinations in the two-quantum $6s^2S_{1/2} \rightarrow 6p^2P_{3/2} \rightarrow 7s^2S_{1/2}$ transition, are measured after a small background signal subtraction. As the four lines are of nearly identical width, either the

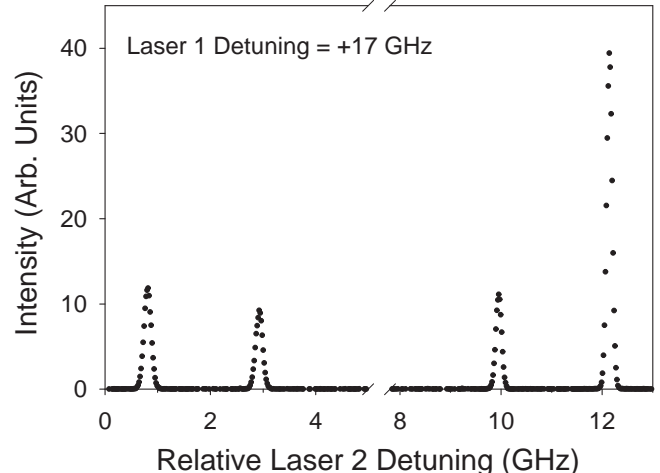


FIG. 4: Illustrative scan of the four hyperfine resonances associated with far-off-intermediate-level resonance of the $6s^2S_{1/2} \rightarrow 7s^2S_{1/2}$ transition. The relative detuning label on the abscissa indicates that the absolute zero of the scan is not specified, but that the relative resonance separations correspond to the detuning differences given in the figure. On the other hand, the detuning indicated in the graph body refers to the hyperfine-averaged $6s^2S_{1/2} \rightarrow 6p^2P_{3/2}$ transition frequency (see text).

integrated area under the line, or the peak amplitude, can in principle be utilized as a measure of line intensity. Although both quantities produce similar results for the various intensity ratios, we choose the amplitude comparison to avoid distortion of the ratios associated with residual non-uniformity in the laser frequency scan rate.

Uncertainties in the peak ratio determinations comes from a combination of photon counting statistics, fluctuations in the thermal lab environment, and laser power variations. While beam power just before the cell show very small changes (< 0.1 percent), the cell entrance window, which has no antireflection coating, can act like an etalon with reflection/ transmission varying somewhat with laser frequency. A simple estimate, as well as auxiliary experimental tests, show that with a characteristic laser 2 frequency change of 2 GHz between peaks corresponding to different F', the cell window transmission never changes by more than about 1 percent. The total uncertainties in the ratios are obtained by adding contributions in quadrature.

IV. RESULTS AND DISCUSSION

Initial tests showed two-quantum-induced fluorescence signals growing strongly with decreasing detuning, in agreement with theoretical predictions. Since the absolute fluorescence signal intensity is not very reproducible from day to day, we keep fluorescence signals roughly

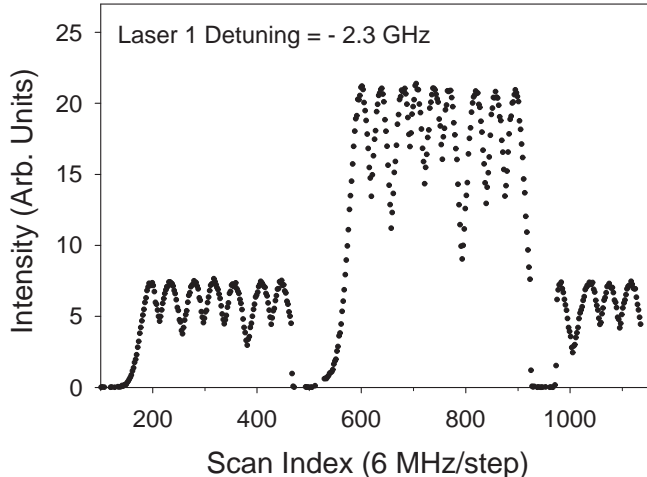


FIG. 5: Typical data showing repeated scans of two hyperfine levels, in this case the transitions initiating in the lower $F = 3$ level. This data illustrates the temporal stability of the apparatus for the purposes of measuring relative intensity ratios. The scan index refers to a single step in the frequency scan (approximately 6 MHz) as the laser is scanned back and forth over the hyperfine resonances. The detuning indicated in the graph body refers to the hyperfine-averaged $6s^2S_{1/2} \rightarrow 6p^2P_{3/2}$ transition frequency (see text).

constant (for example by adjustment of the monochromator slit width), and concentrate on the relative intensity of the various hyperfine transition resonances. With the laser 1 frequency set and laser 2 scanned, four fluorescence peaks are observed corresponding to different $F = 3,4$ to $F' = 3,4$ combinations in the $6s^2S_{1/2} \rightarrow 6p^2P_{3/2} \rightarrow 7s^2S_{1/2}$ two-quantum transition. A characteristic scan over these resonances are illustrated in Figure 4. We should emphasize here that, in all experimental results, detunings refer to the hyperfine-averaged $6s^2S_{1/2} \rightarrow 6p^2P_{3/2}$ transition frequency [36]. Since the hyperfine energy separation in the lower ground level is several times larger than in the final $7s^2S_{1/2}$ level - the spectral signal consists of two doublets separated by the ground level hyperfine splitting. The intensity ratios are carefully determined for pairs of transitions originating from a common lower level, i.e. those starting at $F = 4$, and then those starting at $F = 3$. Such ratios are insensitive to the population in the ground state hyperfine structure sublevels. As already mentioned, the amplitudes of the fluorescence peaks rather than their integrated areas are used as transition probability measures and their ratio taken. Several consecutive scans over each line center are made, in order to assure consistency of the measurements. Occasional records, showing noticeable drifts in values within the series are rejected. Typical scan results are illustrated in Figure 5. The peak regions are fitted to a parabolic line shape and the maximum signal values determined by the fit. After subtraction of the back-

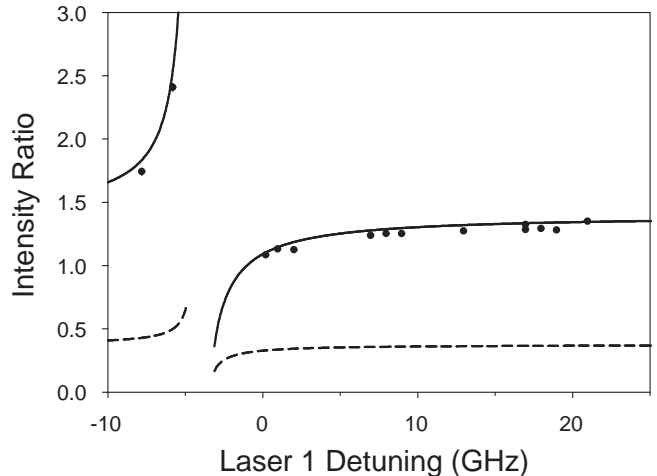


FIG. 6: Spectral variations of the measured intensity ratios of the $F = 4 \rightarrow F' = 3$ to the $F = 4 \rightarrow F' = 4$ hyperfine transition. The solid line represents the theoretical prediction, calculated as described in the text. The dashed curve represents the theoretical prediction, but ignores interference among the two photon hyperfine transition amplitudes. The laser 1 detuning in this figure is referenced to the hyperfine averaged line center.

ground, which consists of dark counts and stray light, the resulting derived values are used for amplitude ratio evaluation. For larger detunings (hyperfine structure splitting \ll detuning \ll fine structure splitting) these values are expected to approach 1.4 and 3, as mentioned earlier. Our experimental data illustrating these effects is shown in Fig. 6 and Fig. 7.

When the laser 1 detuning from a resonance transition becomes comparable with the $6p^2P_{3/2}$ hyperfine splitting the ratios may deviate from the asymptotic values substantially. Transitions populating the $F' = 4$ level dominate over those ending in the $F' = 3$ level when the virtual level is on the higher frequency side of the $6p^2P_{3/2}$ level, and vice versa, while the transition amplitude interference causes the intensity ratios to strongly tend in opposite directions when resonance is approached. In general, although a more complicated behavior of the probability ratios are expected in, for example, an ultracold (due to resolution of individual intermediate hyperfine levels) atomic gas, quantum interference effects in the transition probabilities are clearly demonstrated here as well. This is emphasized by the dashed lines in the figures. These lines correspond to ignoring interferences between the hyperfine transition amplitudes, and directly combining transition probabilities.

Although the experimental data follow quite closely the trends predicted on the basis of the simple model presented here, there are systematic deviations of a few percent between the experimental data and the theoretical predictions. Several possible sources of discrepancy were considered. First, considering the theoretical model

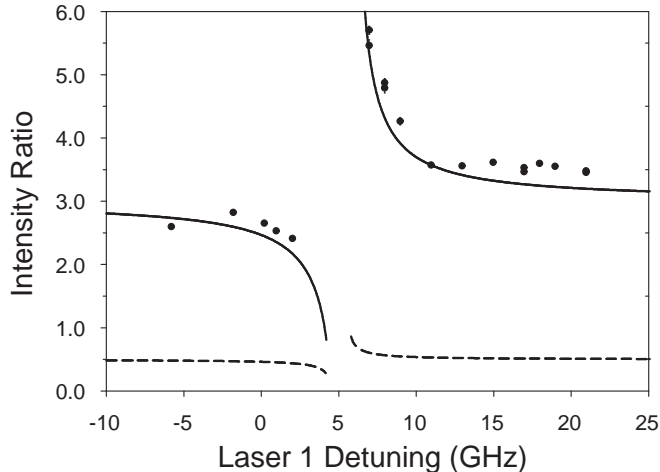


FIG. 7: Spectral variations of the measured intensity ratios of the $F = 3 \rightarrow F' = 4$ to the $F = 3 \rightarrow F' = 3$ hyperfine transition. The solid line represents the theoretical prediction, calculated as described in the text. The dashed curve represents the theoretical prediction, but ignoring interference among the two photon hyperfine transition amplitudes. The laser 1 detuning in this figure is referenced to the hyperfine averaged line center.

used, we emphasize that the main approximations are (a) neglect of contributions of the reverse time-ordering of the two photon transition amplitude, and (b) neglect of transition amplitudes via the energetically distant $6p^2P_{1/2}$ level. Estimates readily show that these contribute negligibly, for the detunings considered here, and at the level of the precision of the measurements. Far off resonance transitions due to more energetically distant np multiplets similarly contribute at a negligible level in comparison with the discrepancies. It further seems unlikely that there are significant variations of the reduced transition matrix elements on the scale of the present experiments. A number of experimental artifacts were also considered. These include imperfectly perpendicular laser beam polarizations and saturation effects in the two photon transition rate. However, it proves difficult to reconcile the discrepancies within reasonable estimates of these effects. The most likely explanation for the few percent differences between the measurements and the theoretical predictions comes from effects of the broad spectral profile of the diode lasers used in the experiments. Although the main output of the diode lasers is generally within a bandwidth \sim MHz, there is a weak and broad spectral plateau. This plateau can be spectrally structured because of low, but not negligible levels of mode competition in the external cavity diode lasers, especially at the spectral edges of the tuning range of the lasers. Mode instability in fact becomes quite evident for the nominal 1470 nm diode laser at detunings somewhat outside the range of than those used in the present experiments. Quantifying these issues is challenging without

recourse to a near infrared sensitive spectrum analyzer, but the scale of the instabilities we observe is in fact consistent with the spectral trend and size of the observed discrepancies.

V. PEDAGOGICAL PERSPECTIVES

The research described in our previous reports [17–22], and in the present paper, form the basis for an excellent set of projects suitable for advanced undergraduate physics laboratories. These projects are based on atomic two-photon, two-color experiments in which quantum interferences play an important role in the observed transition rate. For these experiments there are two types of interference effect. In one, the various amplitudes for intermediate atomic levels contribute coherently to the total transition probability. In the second, the two time-orderings of photon absorption also contribute coherently. In many cases, one of these orderings dominates over the other.

In the work reported here, and in our previous measurements of this type, we have concentrated on studies of alkali atoms. However, this is not in the least a requirement for such studies, and a variety of atomic species, and many molecular ones as well, could be used to provide a variety of new studies to serve as undergraduate research experiences. As such experiments have not been systematically extended to the molecular domain, the roles of multiple rovibrational interferences provide a rich area for interesting, accessible, and original research suitable for undergraduates. In general, the results would also be of sufficient interest to be publishable in traditional physics journals. The projects combine the desirable aspects of experimental technical accessibility, clear physical interpretation, and theoretical analysis within the range of many advanced physics or engineering students. As the theoretical results can be readily parametrized in terms of combinations of atomic or molecular electric dipole transition moments, opportunities also exist for data analysis and fitting. All together, such projects are quite suitable for a single student working with involved faculty, or small teams of advanced undergraduates working together by bringing different skills and inclinations to the projects. It has been our experience with undergraduate and graduate students involved in similar experiments that accurate predictions of line intensity ratios and their variations with detuning can impress even naturally skeptical bright undergraduate physics and engineering students. They also come to appreciate the opportunity to see quantum mechanics going to work and producing excellent results which can be experimentally verified in a student level experiment.

VI. CONCLUSIONS

We have presented measurements of relative transition probabilities for various hyperfine transitions in atomic Cs. The measurements are interpreted through theoretical expressions valid for the spectral detuning range outside the Doppler widths of the atomic transitions, where very good agreement between experiment and theory is obtained. The experimental approach and theoretical results are presented in sufficient detail to guide development of possible undergraduate research projects focussed towards similar atomic or molecular systems.

VII. ACKNOWLEDGMENTS

This work is supported by Central Michigan University and by the National Science Foundation (NSF-PHY-1068159 and NSF-PHY-1606743).

VIII. REFERENCES

-
- [1] G.S.He and S.H.Liu, *Physics of Nonlinear Optics* (World Scientific, Singapore, 1999).
- [2] R.W.Boyd, *Nonlinear Optics* (Academic, San Diego, 1992).
- [3] Y.R.Shen, *The Principles of Nonlinear Optics* (Wiley, New York, 1984).
- [4] Michael A.Nielsen and Isaac L.Chuang, *Quantum Computation and Quantum Information* (Cambridge University Press, Cambridge, 2000).
- [5] Zbigniew Ficek and Stuart Swain, *Quantum Interference and Coherence* (Springer, New York, 2005).
- [6] H. Cao, Lasing in Random Media, in *Waves in Random Media* **13**, R1 (2003).
- [7] William Guerin, Franck Michaud, and Robin Kaiser, Mechanisms for Lasing with Cold Atoms as the Gain Medium, *Phys. Rev. Lett.* **101**, 093002 (2008).
- [8] Harold J.Metcalf and Peter van der Straten, *Laser Cooling and Trapping* (Springer-Verlag New York, 1999).
- [9] F.Biraben, B.Cagnac, and G.Grynberg, Experimental evidence of two-photon transition without Doppler broadening, *Phys. Rev. Lett.* **32**, 643-645 (1974).
- [10] M.D. Levenson and N.Blombergen, Observation of two-photon transition without Doppler broadening on the 3S-5S transition in sodium vapor, *Phys. Rev. Lett.* **32** (1974).
- [11] C.Wieman, G.Flowers, and S.Gilbert, Inexpensive laser cooling and trapping experiment for undergraduate laboratories, *Am. J. Phys.* **63**, 317 (1995).
- [12] K.B. MacAdam, A. Steinbach, and C.Wieman, A narrow-band tunable diode laser system with grating feedback, and a saturated absorption spectrometer for Cs and Rb, *Am. J. Phys.*, **60**, 1098 (1992).
- [13] A.J. Olson, E.J. Carlson, and S.K. Mayer, Two-photon spectroscopy of rubidium using a grating-feedback diode laser, *Am. J. Phys.* **74**, 2218-2239 (2006).
- [14] F.Nez, F.Biraben, R.Felder, and Y.Millerieux, Optical frequency determination of the hyperfine components of the $5S_{1/2}$ - $5D_{3/2}$ two-photon transitions in rubidium, *Opt. Commun.* **102**, 432 (1993).
- [15] T.T. Grove, V. Sanchez-Villicana, B.C. Duncan, S.Maleki, and P.L. Gould, Two-photon two-color diode laser spectroscopy of the Rb $5D_{5/2}$ state, *Phys. Scr.* **52**, 271 (1995).
- [16] R.E. Ryan, L.A. Westling, and H.J. Metcalf, Two-photon spectroscopy in rubidium with a diode laser, *J. Opt. Soc. Am. B* **10**, 1643 (1993).
- [17] S.B. Bayram, M.D. Havey, M.S. Safronova, and A.Sieradzan, Nonlinear optical approach to matrix-element spectroscopy of the $5s^2S_{1/2} \rightarrow 5p^2P_j \rightarrow 6d^2D_j$, transitions in ^{87}Rb , *J. Phys. B: At. Mol. Opt. Phys.* **39**, 1 (2006).
- [18] A.I. Beger, M.D. Havey, R.P. Meyer, Precise measurement of the $5s^2S_{1/2} \rightarrow 5p^2P_j \rightarrow 8s^2S_{1/2}$ two-photon, two-color polarization spectrum in atomic Rb, *Phys. Rev. A* **55**, 3780 (1997).
- [19] R.P. Meyer, A.I. Beger, and M.D. Havey, Precise measurement of relative transition matrix elements of the Na $3s^2S_{1/2} \rightarrow 3p^2P_j \rightarrow 5s^2S_{1/2}$ by two-photon, two-color polarization spectroscopy, *Phys. Rev. A* **55**, 230 (1997).
- [20] M.D. Havey, Light scattering spectroscopy: a new method for determination of atomic matrix elements, *Phys. Lett. A* **240**, 219 (1998).
- [21] S.B. Bayram, M.Havey, M.Rosu, A.Sieradzan, A. Derevianko, and W. R. Johnson, $5p^2P_j \rightarrow 5d^2D_{3/2}$ transition matrix elements in atomic ^{87}Rb , *Phys. Rev. A* **61**, 050502(R) (2000).
- [22] A.Markhotok, S.B. Bayram, A.Sieradzan and M.D. Havey, Precision polarization measurements of the $6s^2S_{1/2} \rightarrow 6p^2P_j$ Rayleigh scattering spectrum in atomic Cs, *J. App. Phys.* **92**, 1613 (2002).
- [23] For a recent review, see A. Derevianko and S. G. Porsev, *Eur. Phys. J. A* **32**, 517 (2007).
- [24] J.S.M. Ginges and V.V. Flambaum, *Phys. Rep.* **397**, 63 (2004).
- [25] C.S. Wood, S.C. Bennett, D. Cho, B.P. Masterson, J.L. Roberts, C.E. Tanner and C.E. Wieman, *Science* **275**, 1759 (1997).
- [26] M.A. Bouchiat and C. Bouchiat, *Rep. Prog. Phys.* **60**, 1351 (1997).
- [27] J. Guena, M. Lintz, and M.A. Bouchiat, *Phys. Rev. A* **71** 042108 (2005).
- [28] M. Lintz, J. Guena, and M.A. Bouchiat, *Eur. Phys. J. A* **32** 525 (2007).
- [29] R.Loudon, *Quantum Theory of Light*, 2nd ed. (Oxford University Press, Oxford, 1992).
- [30] A.A.Radzig, B.M.Smirnov, *Reference Data on Atoms, Molecules and Ions* (Springer, Berlin, 1985).
- [31] Paul W. Brumer and Moshe Shapiro, *Principles of the Quantum Control of Molecular Processes*, Wiley-Interscience, Hoboken, New Jersey (2003).
- [32] J.R. Tolsma, D.J. Haxton, C.H. Greene, R. Yamazaki, and D.S. Elliott, *Phys. Rev. A* **80**, 033401 (2009).

- [33] R. Yamazaki and D.S. Elliott, Phys. Rev. Lett. 98, 053001 (2007).
- [34] C. Cohen-Tannoudji, J. Dupont-Roc, G. Grynberg, Atom-Photon Interactions: Basic Processes and Applications (Wiley, New York, 1992).
- [35] M.E. Rose, Elementary Theory of Angular Momentum (Wiley, New York, 1957).
- [36] D. A. Steck, Cesium D Line Data, Available online at <http://steck.us/alkalidata>.